Proceedings of the 2019 IEEE/ASME
International Conference on Advanced Intelligent Mechatronics
Hong Kong, China, July 8-12, 2019

Decompensation Prediction in Hemodialysis by a Feedback Model as Identified by Miniature Wearable Sensors

Lu Wang, Sardar Ansari, Kayvan Najarian, Kevin R. Ward, Kenn R. Oldham, *Member, ASME/IEEE*

***Abstract*— A simple feedback model for blood pressure regulation is described that incorporates multiple autoregulatory feedback mechanisms, all of which may be monitored by a proposed wearable sensor. The feedback signals measured, either directly or indirectly, are heartrate, peripheral vascular resistance, and compression volume. When examined for trends among hemodialysis patients, sustained reduction in feedback amplitudes below those predicted by the model appears to be strongly associated with later blood pressure decompensation.**

I. Introduction

The body's ability to compensate against stress caused by trauma, illness, and disease can substantially complicate diagnosis and detection of complications in many situations. For example, multiple autoregulatory feedback loops exist to maintain blood pressure at the core and vital organs. As a result, measurements of blood pressure tend to act as a trailing indicator of cardiovascular distress, while feedback behaviors that are much more difficult to monitor may be changing rapidly. Thus, early prediction of hemodynamic decompensation, or a rapid decrease in blood pressure, has remained difficult to achieve, due to limitations on physiological monitors and patient-to-patient variability.

One setting in which hemodynamic decompensation is relatively common is hemodialysis. Over 25% of hemodialysis sessions have been reported to be complicated by decompensation or other symptoms of intradialytic hypotension (IDH), with significant impact on morbidity [1]. Several prior studies have attempted to predict when IDH will occur, either by classifying patient risk factors prior to hemodialysis [2] or applying statistical and/or machine learning techniques to existing physiological measures taken during hemodialysis, such as blood pressure (BP), the electrocardiogram (ECG), pulse photoplethysmogram (PPG), and/or heart rate variability (HRV) data [3] [4] [5] [6] [7]. However, sensitivity and specificity of these predictors remains limited. Several attempts at decompensation prediction in other clinical settings have been based on similar strategies, such machine learning application to PPG waveforms to create a compensatory reserve index (CRI) [8].

In contrast, this work seeks to isolate various components of cardiovascular autoregulation to construct models of interacting feedback dynamics. Over time frames of minutes to hours, major feedback signals regulating BP are considered to include heartrate, compression volume, and peripheral vascular resistance [9]. Importantly, we have recently created a wearable sensor system for continuously measuring peripheral vascular resistance [10] [11], which is otherwise available on a continuous basis only in specialized clinical settings. The sensor also provides high-fidelity tracking of small peripheral artery pressure fluctuations, which we have also proposed for analysis in predicting IDH or assessing other cardiovascular events such as hemorrhage [12] [13] [14].

Here, we hypothesize that incorporating peripheral vascular resistance into feedback models for cardiovascular autoregulation can increase understanding of decompensation and improve IDH prediction. This effort differs from previous attempts to model feedback dynamics primarily in the availability of additional feedback signals from non-invasive sources, and also the examination of variation in feedback over time during the complex medical intervention of hemodialysis. Prior works on autoregulation modeling have primarily examined feedback dynamics identification under comparatively controlled conditions [9] [15] [16].

This paper will thus describe a simple feedback model for cardiovascular autoregulation, describe how feedback signals were tracked, and perform parameter and state for hemodialysis patients. Certain estimator error behaviors will be associated with later decompensation during hemodialysis.

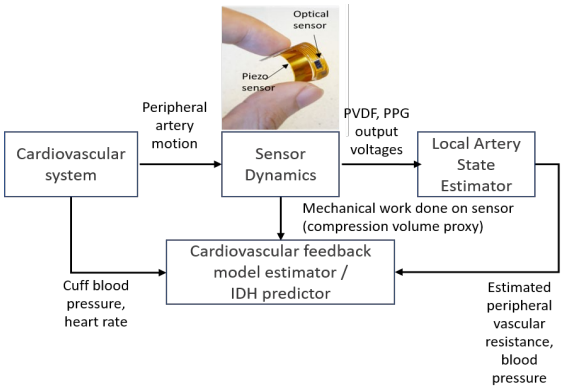

Figure 1. Conceptual framework for decompensation prediction during hemodialysis: signals associated with blood pressure autoregulation are monitored directly or indirectly using a simple wearable sensor and used to identify parameters in an abstracted model for feedback processes within the body; signals from the estimator are used to predict later decompensation.

*Research supported by National Science Foundation, award CMMI-1562254, Coulter Foundation, Michigan Translational Research and Commercialization (M-TRAC) program, and Michigan Center for Integrative Research in Critical Care (M-CIRCC).

L. Wang and K.R. Oldham are with the University of Michigan Department of Mechanical Engineering, Ann Arbor, MI 48109 USA. (phone: 734-615-6327; e-mail: oldham@umich.edu).

S. Ansari is with the Department of Emergency Medicine, University of Michigan, Ann Arbor, MI 48109 USA.

K. Najarian is with the Department of Computational Medicine and Bioinformatics and Department of Emergency Medicine, University of Michigan, Ann Arbor, MI 48109 USA.

K. Ward is with the Department of Emergency Medicine, Department of Biomedical Engineering, and Michigan Center for Integrative Research in Critical Care, University of Michigan, Ann Arbor, MI 48109 USA.

II. Feedback Model

The feedback model used for IDH prediction was constructed from a simple nonlinear cardiovascular monitor and a set of linear low-pass filters representing feedback processes. While a major simplification of full cardiovascular dynamics, the selection of models was intended to balance the range of autoregulatory phenomena to be monitored with the number of parameters to be identified.

The cardiovascular system was modeled as a simple fluidic resistance and capacitance driven by a pressure source, with resistance and input pressure influenced by "control inputs" (vector **u**) of heart rate, u_1, mechanical work done per beat by the artery to the sensor (a proxy for compression volume), u_2, and peripheral vascular resistance, u_3:

$$\dot{P} = f(P, \mathbf{u}, d) = l_1 u_1 u_2 - l_2 \frac{P}{u_3} + l_3 d \qquad (1)$$

where P is blood pressure as would be measure using a conventional blood pressure (BP) cuff or arterial line; l_1 is a parameter to scale the combined pressure forcing input of heart rate and supposed compression volume; l_2 is a parameter for first order dynamics produced by total hemodynamic capacitance and resistance, assumed to be inversely dependent on peripheral vascular resistance; and d is a net disturbance from external factor (activity level, hemodialysis effects, etc.).

Feedback dynamics were modeled as responding to the difference between blood pressure and some supposed internal reference pressure, P_r, with a time delay represented as a linear low-pass filter. In addition, the disturbance was assumed to be able to affect the feedback signals directly, with comparable response time. The resulting simple feedback model becomes, in Laplace space,

$$U_i(s) = \frac{b_i}{s+a_i}(P_r - P(s)) + \frac{c_i}{s+a_i} D(s) \qquad (2)$$

where b_i is the feedback gain to pressure, a_i is the first-order filter parameter, and c_i is the coupling parameter to external disturbance for the i-th control input.

Measurements y_1, y_2, and y_3 were assumed to be available for each of the three feedback signals, though fidelity and sampling rate could differ based on source of measurement, as described in more detail in Section III. In addition, a measure of BP, y_4, was assumed to be at least intermittently available. The resulting feedback system with measurement locations is summarized in block diagram form in Fig. 2.

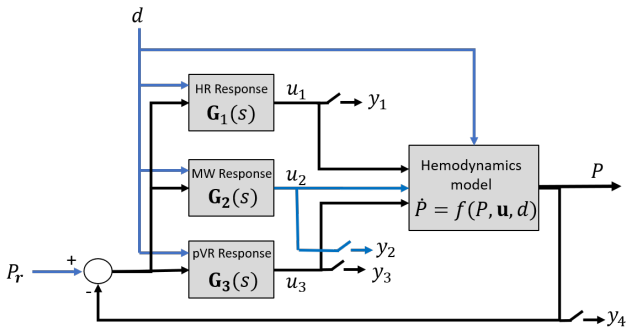

Figure 2. Individual low-order approximations of cardiovascular behavior are connected via feedback between blood pressure variation and supposed autoregulatory (i.e. feedback control) signals.

III. Data Collection

A. Hardware

Peripheral arterial behavior was monitored using sensor data from a PPG and a compliant piezoelectric polymer (polyvinylidene difluoride, or PVDF) worn on the fingers. Details of PVDF sensor design and usage for tracking peripheral vascular resistance have been previously reported in swine subjects in [10] and [11]. In addition to wearable sensor information, conventional cuff blood pressure (BP) was recorded approximately every 15 minutes.

B. Data Collection

Sensors were applied to 110 hemodialysis patients in the inpatient dialysis unit at the University of Michigan Hospital, from which 91 complete data sets were successfully collected; 50 data sets have been fully processed at the time of writing and are reported on in this manuscript. The PVDF ring was applied within approximately ten minutes of the beginning of hemodialysis, and ring tension was adjusted manually to produce a clear PVDF waveform. For some patients, readjustment was performed if the sensor was dislodged due to patient activity. Other than those cases, both patients and care providers were kept blind to signal behavior during the dialysis session. All data collection was performed under IRB-approved human subject protocol UM HUM00112816.

C. Signal Processing

Raw voltage versus time data from the PVDF and PPG sensors was processed to provide measures of relative change in major autoregulatory cardiovascular behaviors. First, heart rate (labeled *HR*) was extracted from peak values of the PPG signal. Second, a measure was sought to approximate compression volume at the heart. A proxy was selected as the mechanical work (labeled *MW*) done by peripheral arterial motion on the PVDF ring within each cardiac cycle. This is only hypothetically related to cardiovascular health but chosen as at least partially representative of the heart's work capacity during individual heartbeats. Third, peripheral vascular resistance (labeled *pVR* for conciseness, not to be confused with pulmonary vascular resistance often labeled PVR) was estimated using methods previously reported [10] [11].

It is important to note that peripheral vascular resistance estimation has not yet been directly validated on human subjects, so a major assumption in this work is that the methods applied to swine subjects translate to humans. In brief, a simple model for tissue viscoelasticity between the artery and PVDF and PPG sensors is identified using a fast-time-scale (200 Hz sampling rate) extended Kalman filter (EKF) to produce state estimates of changes in local artery radius and internal blood pressure. pVR changes are derived from radius change. This approach has shown good agreement (<5% average absolute error) between estimated vascular resistance changes and those measured by gold standard arterial catheterization in swine [10].

An adjustment to prior methods done in this work was to adjust sensor noise weighting fort the local artery model EKF based on pulse transit time (PTT) between PPG and PVDF locations. When PTT was within a specified margin, PVDF and PPG signals were incorporated into the EKF as normal. When PTT deviated from the expected margin, one or both the

sensors was assumed to be disturbed by patient movement, and the EKF was applied during that cardiac cycle based on a substantially increased noise variance (i.e., placing substantially greater trust in the model vs. measurements).

For each subject, proposed feedback signals were normalized to a 0 to 1 scale based on a set maximum (subscript *max*) and minimum (subscript *min*) plausible range for those signals, to simplify scaling between parameters.

$$y_1 = \frac{HR - HR_{min}}{HR_{max} - HR_{min}}, \tag{3}$$

$$y_2 = \frac{MW - MW_{min}}{MW_{max} - MW_{min}} \tag{4}$$

$$y_3 = \frac{\widehat{pVR} - pVR_{min}}{pVR_{max} - pVR_{min}} \tag{5}$$

where y_1 is the normalized magnitude of heartrate, y_2 is the normalized magnitude of work being transmitted to the compliant sensor, and y_3 is the normalized magnitude of peripheral vascular resistance calculated by the local artery model EKF. Average values for the first 30 seconds for measured signals were used as initial conditions where relevant during further parameter identification.

A byproduct of the peripheral vascular estimation process is to provide a continuous estimate of blood pressure (BP). While the PVDF sensor cannot directly measure blood pressure, an internal state in the vascular resistance model is the fluctuation internal artery pressure over time. Piezoelectric sensing of this type is vulnerable to long term drift, but when provided periodically with a reference BP measurement (i.e. from a BP cuff), the sensor and estimator have been found to track BP measured by conventional means, P_{cuff}, with approximately 10% error over a time period of several hours. In the hemodialysis setting, BP cuff measurements are available approximately every 15 minutes, while the continuous but lower-confidence measure from the sensing ring, labeled $\hat{P}_{pVR}$, was used at other sampling points. BP output, y_4, is thus provided by one of two potential sources:

$$y_4 = \begin{cases} P_{cuff} + v_{4,cuff}, & P_{cuff} \neq 0 \\ \hat{P}_{pVR} + v_{4,pVR}, & P_{cuff} = 0 \end{cases} \tag{6}$$

where v_4 is a measure of noise or accuracy error in the signals, varying with the source (*cuff* vs. pVR estimator).

Finally, "disturbance", d, to the cardiovascular system was treated as being partially generated by activity level. A crude approximation of patient activity level, labeled $\bar{d}$, was taken from the unfiltered mean PVDF amplitude as computed from a rolling averaged of 30 seconds, as large amplitude variations in PVDF output are associated with motion artifacts. Standard deviation of the PVDF signal over that period was used to compute a disturbance variance for the cardiovascular feedback model state estimator described below.

IV. Parameter Identification and State Estimation

Parameter identification and state estimation were done simultaneously using an augmented extended Kalman filter. First, dynamics in (1) and (2) were converted to discrete time with states collected in state vector $\mathbf{q} = [P \; u_1 \; u_2 \; u_3]^T$. Unknown parameters from (1) and (2) were collected in a potentially time-varying parameter vector,

$$\boldsymbol{\theta} = [P_r \; \lambda_1 \; \lambda_2 \; \lambda_3 \; \alpha_1 \; \beta_1 \; \gamma_1 \; \alpha_2 \; \beta_2 \; \gamma_2 \; \alpha_3 \; \beta_3 \; \gamma_3]^T \tag{7}$$

where λ_1, λ_2, and λ_3 are discrete-time analogs to l_1, l_2, and l_3 from (1), and α_i, β_i, and γ_i terms are discrete-time analogs to a_i, b_i, and c_i from (2). State and parameter vectors were combined to create a single plant model for the estimator based on estimated states, $\hat{\mathbf{q}}$, and estimated parameters, $\delta\hat{\boldsymbol{\theta}}$, where δ indicates that parameters are estimated as their perturbation from a set of nominal baseline values:

$$\begin{bmatrix} \hat{\mathbf{q}}^{\mathbf{0}}(k+1) \\ \delta\hat{\boldsymbol{\theta}}^0\,(k+1) \end{bmatrix} = \begin{bmatrix} f(\hat{\mathbf{q}}(k), \hat{\boldsymbol{\theta}}(k), \bar{d}(k)) \\ \alpha\mathbf{I} \cdot \delta\hat{\boldsymbol{\theta}}(k) \end{bmatrix} \tag{8}$$

Here, α is a decay parameter; conceptually, time-varying parameters are being treated as though they slowly perform a random walk around their nominal values driven by external disturbances, to be tracked by this augmented EKF. Superscript $^{\mathbf{0}}$ denotes *a priori* estimates generated from *a posteriori* estimates from the previous time step.

Given the measurements identified in Section III.C., the output vector of the physical system is simply

$$\mathbf{y} = \mathbf{q} + \mathbf{v} \tag{9}$$

where $\mathbf{v}$ is a vector of the noise in each measurement, and thus the estimated system output is simply $\hat{\mathbf{y}} = \hat{\mathbf{q}}$.

A posteriori state and parameter updates are then generated in the common observer form

$$\begin{bmatrix} \hat{\mathbf{q}}(k+1) \\ \delta\hat{\boldsymbol{\theta}}\,(k+1) \end{bmatrix} = \begin{bmatrix} \hat{\mathbf{q}}^{\mathbf{0}}(k+1) \\ \delta\hat{\boldsymbol{\theta}}^0\,(k+1) \end{bmatrix} + \mathbf{L}(\hat{\mathbf{y}}(k) - \mathbf{y}(k)) \tag{10}$$

where $\mathbf{L}$ is a gain matrix calculated by existing extended Kalman filter methods (in this case, the procedure in [17]) based on linearization of dynamics in (8) about the current state estimates and iterative generation of error covariance and estimator gain matrices.

V. Results

A. Peripheral Vascular Resistance Observations

Before discussing feedback model estimator results, it is useful to describe representative behavior of peripheral vascular resistance tracking as implemented based on the authors' previous methods from [11]. It was observed that consistency of inferred peripheral vascular resistance alone was a strong negative predictor of intradialytic hypotension. Among patients where inferred vascular resistance varied less than ±50%, only 5% of sessions resulted in substantial decompensation (set as a drop >25% of nominal BP) and/or had patient reported symptoms of distress. In contrast, over 30% of cases with large vascular resistance fluctuations were associated with a drop in BP and over 30% with reported symptoms (some cases overlapping). Examples of patients with small and large inferred vascular resistance changes are shown in Fig. 2 with corresponding BP fluctuations.

Our interpretation of these observations is that fluctuations in peripheral vascular resistance may be indicative of compensatory response that will eventually result in decompensation, but vascular resistance change alone is not necessarily tied to decompensation. Rather, vascular

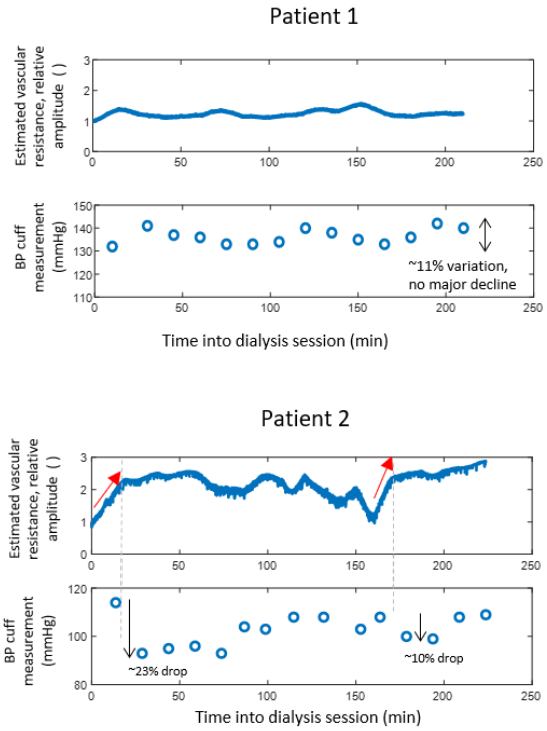

Figure 3. Mild variation in inferred or estimated peripheral vascular resistance, as in Patient 1 above, is very rarely associated with large BP fluctuations, while large patients experiencing large BP tend to exhibit prior peripheral vascular response, as in Patient 2 above.

resistance change may also occur as part of a compensation process that is sustainable, at least over the several-hour period of a hemodialysis session, or as a response to other disturbances, such as change in activity level. The need to distinguish unsustainable compensatory response from other cases where pVR fluctuated thus partially motivated the feedback modeling described above.

B. Estimator calibration and representative outputs

Several items were calibrated in the model and extended Kalman filter using an initial training set of 20 patients (from 50 overall). These included the selection of 30 seconds for averaging of PVDF noise to compute $\bar{d}$ and nominal values for $\boldsymbol{\theta}$. Rolling average duration was selected to minimize mean absolute error in $(\hat{\mathbf{y}} - \mathbf{y})$ for this training data set, while nominal values for $\boldsymbol{\theta}$ were set based by a brute force search to minimize total absolute error $(\hat{\mathbf{y}} - \mathbf{y})$ across all 20 subjects with a single set of values, as a starting point from which parameters would then diverge on an individual basis during EKF application.

Fig. 2 shows a sample set of estimation results for a patient with significant BP variation but without decompensation (BP remained above that at the beginning of hemodialysis). The estimator is only modestly effective in predicting blood pressure trends, with errors up to 30 mmHg, when comparing estimates for pressure to the intermittent cuff measurements. This is likely because the disturbances that may be perturbing blood pressure are largely unknown. However, the feedback signals are much more closely predicted by the estimator. This is in part due to substantial autocorrelation of those

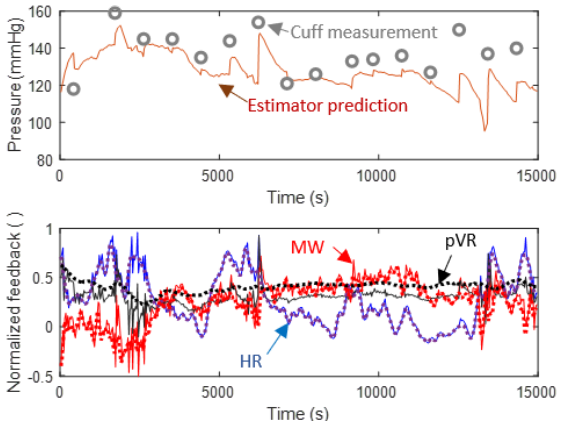

Figure 4. Blood pressure predictions from the EKF provide only modest tracking of trends in BP during hemodialysis, as for this sample patient, though feedback signals are more effectively predicted (solid: from EKF; dashed: from physiological sensing). BP prediction errors tend to be associated with sustained error between prediction and measurement of one or more of the feedback signals.

signals with themselves, but also aided by the continuous feedback measurements and their interrelationship. Notably for the sample patient in Fig. 4, "overperformance" of BP relative to the model in the latter portion of hemodialysis is associated with an "overperformance" of one of the feedback signals: in this case peripheral vascular resistance remained higher than anticipated by the estimator based on feedback parameters being identified since the start of the session.

To further evaluate apparent feedback effectiveness, a control chart-like analysis was performed, with sample results shown in Fig. 5 for the patients previously discussed in Fig. 3. In Fig. 5, solid lines denote the mean error in each of the feedback signals over the time between BP cuff measurements (i.e. $\underset{k_p \le k < k_{p-1}}{\text{mean}} (\hat{u}_i - u_i)$, where k_p and $k_{p\text{-}1}$ represent the current and previous time steps at which BP cuff data was taken), ○ and x points indicate the maximum and minimum prediction errors at a single time points during each period, and dashed lines represent the expected standard deviation in feedback signals, approximated by the mean of corresponding diagonal terms in the error covariance matrix.

Among the training data set of 20 patients, it was observed that large but short duration errors were not strongly correlated with BP fluctuations. However, sustained positive error (predicted feedback magnitude larger than measured feedback magnitude, or "underperforming" expectations) in one or more feedback signals was observed preceding decompensation events. For example, for Patient 1, who had little variation in BP cuff measurements, mean feedback error was very close to zero; what error was present was also largely negative, implying stronger autoregulatory response than predicted by the model, and small relative to the expected range of deviation obtained from the EKF. In contrast, for Patient 2, who experienced large BP drops early in the session, feedback error was consistently positive and nearly a full standard deviation above that predicted by the estimator throughout the first two hours of hemodialysis.

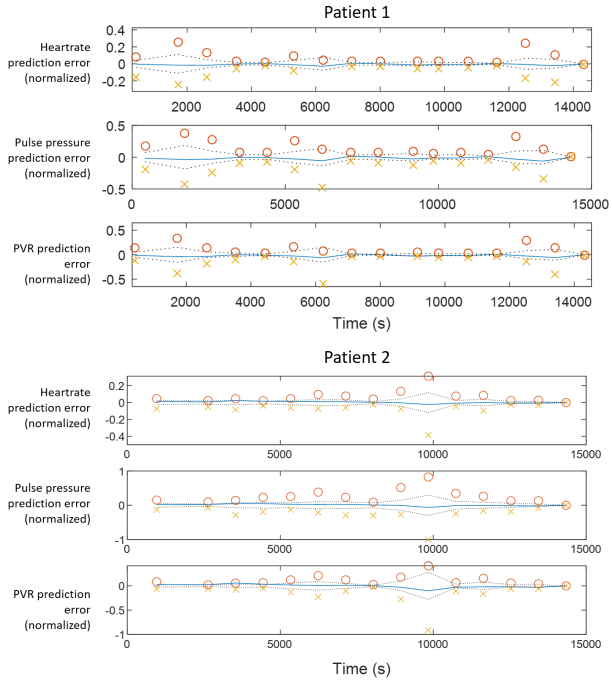

Figure 5. For patients from Fig. 3, comparison of normalized prediction error (solid lines) for the three feedback signals in the dynamic BP model, averaged over time periods between BP cuff measurements, compared to worst case single time point prediction errors (○: maximum, x: minimum) and approximate modeled standard deviation of those signals, as obtained from the EKF error covariance matrix. For Patient 1, error is small relative to anticipated deviation and tends negative (predicted response less than observed), while for Patient 2, who experienced large drops in BP, error tended positive (measured feedback lagging predicted levels) by nearly a full standard deviation.

C. Decompensation Prediction

Based on qualitative observations in Sections V.A. and V.B., decompensation prediction criteria were pursued based on thresholds for peripheral vascular resistance, mean feedback signal error, and time duration exceeding threshold values. A crude brute force evaluation of candidate thresholds and duration was performed on the 20 patient training set, to maximize the product of sensitivity and specificity in predicting decompensation. Decompensation was formally defined as a BP reduction >25% from baseline.

Best performance was found obtained for thresholds of pVR exceeding 165% of its initial value and mean feedback error exceeding 75% of predicted standard deviation, for a duration of 90 seconds. Under these criteria, sensitivity to future decompensation was 100% and specificity was 88% for the training data set, and 100% and 84% for the full 50 patient sample. Fig. 6 shows a sample ROC for the full sample when varying pVR threshold, with feedback error and duration are fixed. Area under the curve was 0.904. On average, thresholds were exceeded 59 minutes prior to decompensation measurement with the BP cuff.

A sample progression as observed under this approach to decompensation prediction is shown in Fig. 7, for a patient experiencing decompensation among the validation data set. Inferred peripheral vascular was elevated in this patient almost immediately and remained elevated throughout the session. Prediction error for feedback signals likewise

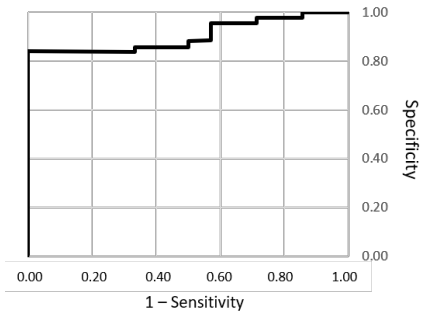

Figure 6. ROC for prediction of decompensation (25% BP reduction from baseline) for varying peripheral vascular resistance thresholds accompanied by violation of feedback signal prediction error for at least 90 seconds.

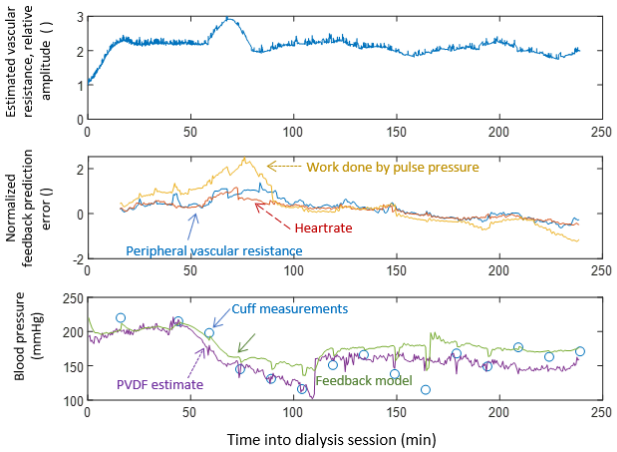

Figure 5. (Top) Ratio of inferred peripheral vascular resistance to its initial value; (Middle) errors in measure feedback signals (positive values mean larger predicted value than measured), normalized by approximate standard deviation from EKF; (Bottom) BP trajectories, including values PVDF sensor as byproduct of pVR estimation and from the feedback model.

gradually increased during the first hour of hemodialysis, exceeding the error threshold criteria approximately 30 minutes into the session, at which point future decompensation is predicted to occur. In this case, weak mechanical work done to the sensor, perhaps interpretable as lagging pulse pressure, was the primary indicator of insufficient cardiovascular response to blood pressure changes, though additional deviation in both pVR and HR occurred approximately 60 minutes into the session. Formal decompensation criteria were not met until 89 minutes into the session, though BP decline had likely also begun to occur at approximately 60 minutes. The patient received a fluid bolus shortly thereafter, though if this was responsible for stabilizing BP, the estimator would suggest the bolus required tens of minutes to take effect.

D. Discussion

Results of this study to date are limited by relative rareness of quantifiable BP decompensation (as opposed to diagnosis based on symptoms or subjective observations) and reliance on substantial qualitative interpretation as gold standard measures of phenomena used in modeling are not available in the hemodialysis setting. As noted at their introduction, feedback measures are not individually validated in humans, and much support for their relevance remains subjective. Furthermore, dynamic models used to represent feedback

dynamics are knowingly simplistic relative to real physiology. Even then, the large number of variables substantially limits trust in individual identified parameters, though outputs and system states seem to be reasonably predictable.

Nonetheless, the observed relationships between trends in model and estimator outputs and BP behavior for hemodialysis patients suggests that there is potential utility in the framework of control system analysis to the hemodynamic decompensation problem. We would interpret key features of the approach being the ability to adapt dynamics to individuals and thus account for variation and interconnectedness in relative timing of physiological phenomena. Differing delays in different signals for different individuals, in particular, can be hard to capture with other statistical methods. Future work will apply these methods to patients with more comprehensive physiological monitors, such as arterial lines, and on larger patient populations.

VI. Conclusions

This work uses a set of approximate measures of feedback signals important for blood pressure autoregulation over minute to hour timeframes to predict future decompensation in hemodialysis patients. Formally, BP drops >25% were predicted with good sensitivity and specificity using inferred changes in peripheral vascular resistance combined with prediction errors between anticipated magnitude of autoregulatory feedback signals and their measured values, as generated by a comparatively simple hemodynamic and autoregulatory dynamics model. Parameter identification and state estimation were performed concurrently on the model using an extended Kalman filter. Results are limited by lack of gold standard physiological data in the hemodialysis setting to better validate measurement accuracy, model structure, and physiological interpretations. However, relative success in decompensation prediction may suggest importance of capturing relative delay and interaction between feedback phenomena at an individually-identified level to predict hemodynamic decompensation events.

Acknowledgment

The authors thank Dr. Michael Heung, Amanda Pennington, Alexander Pan, Hamid Helmi, Kaiwen Lin, Dr. M. Hakam Tiba, and Brendan McCracken for their assistance in testing of the PVDF/PPG sensors and collection of data.

References

[1] W. Bradshaw, P. Bennett, A. Hutchinson, C. Ockerby and P. Kerr, "Preventing intradialytic hypotension: translating evidence into practice," *Nephrology Nursing Journal,* vol. 44, no. 2, pp. 131-139, 2017.

[2] L. Gabutti, M. Machacek, C. Marone and P. Ferrari, "Predicting intradialytic hypotension from experience, statistical models, and artificial neural networks," *Journal of Nephrology,* vol. 18, no. 4, pp. 409-416, 2005.

[3] R. Mendes, S. Santos, D. Dorigo, G. Mansoor, S. Crowley, W. White and A. Peixoto, "The use of peridialysis blood pressure and intradialytic blood pressure changes in the prediction of interdialytic blood pressur in hemodialysis patients," *Blood Pressure Monitoring,* vol. 8, no. 6, pp. 243-248, 2003.

[4] K. Solem, B. Olde and L. Sornmo, "Prediction of intradialytic hypotension using photoplethysmography," *IEEE Transactions on Biomedical Engineering,* vol. 57, no. 7, pp. 1611-1619, 2010.

[5] F. Sandberg, R. Bailon, D. Hernando, P. Laguna, J. Martinez, K. Solem and L. Sornmo, "Prediction of intradialytic hypotension using PPG and ECG," in *Computing in Cardiology*, Zaragoza, Spain, 2013.

[6] C.-J. Lin, C.-Y. Chen, P.-C. We, C.-F. Pan, H.-M. Shih, M. Huang, L.-H. Chou, J.-S. Tang and C.-J. Wu, "Intelligent system to predict intradialytic hypotension in chronic hemodialysis," *Journal of Formosan Medical Association,* vol. 117, no. 10, pp. 888-893, 2018.

[7] V. Chan, L. Chan and D. Chow, "Oxygen saturation and heart rate variations as predictors of intradialytic hypotension," *Nephrology Nursing Journal,* vol. 45, no. 1, pp. 53-61, 2018.

[8] J. Janak, J. Howard, K. Goei, R. Weber, G. Muniz, C. Hinojosa-Laborde and V. Convertino, "Predictors of onset of hemodynamic decompensation during progressive central hypovolemia," *Shock,* vol. 44, no. 6, pp. 548-553, 2015.

[9] V. McLoone, Modeling of Long and Short Term Blood Pressure Control Systems, Maynooth, Ireland: Thesis: National University of Ireland Maynooth, 2014.

[10] L. Wang, S. Ansari, D. Slavin, K. Ward, K. Najarian and K. Oldham, "Non-invasive vascular resistance monitoring with a piezoelectric sensor and photoplethysmogram," *Sensors and Actuators A: Physical,* vol. 263, pp. 198-208, 2016.

[11] L. Wang, S. Ansari, K. Najarian, K. Ward and K. Oldham, "Estimation of peripheral artery radius using non-invasive sensors and Kalman filtering of local dynamics," in *Proc. American Control Conference*, Seattle, WA, 2017.

[12] S. Ansari, N. Farzaneh, M. Heung, K. Oldham, H. Derksen and K. Najarian, "Real-time detection of intradialytic hypotension using a novel polyvinylidene fluoride based sensor," in *IEEE Biomedical Health Informatics Conf.*, 2016.

[13] S. Ansari, S. Molaei, K. Oldham, M. Heung, K. Ward and K. Najarian, "An extended Kalman filter with inequality constratints for real-time detection of intradialytic hypotension," in *Proceedings of IEEE International Conference of the Engineering in Medicine and Biology Society*, Seogwipo, South Korea, 2017.

[14] S. Ansari, D. Slavin, M. Tiba, H. Derksen, K. Ward, K. Oldham and K. Najarian, "A novel portable polyvinylidene fluoride based sensor for detection of hemorrhage," *Circulation,* vol. 132, p. A18257, 2015.

[15] R. Mukkamala, J.-O. Hahn, O. Inan, L. Mestha, C.-S. Kim, H. Toreyin and S. Kyal, "Toward ubiquitous blood pressure monitoring via pulse transit time," *IEEE Transactions on Biomedical Engineering,* vol. 62, no. 8, pp. 1879-1901, 2015.

[16] K. Lau and A. Figeuroa, "Simulation of short-term pressure regulation during the tilt test in a coupled 3D-0D closed-loop model of the circulation," *Biomechanics and Modeling in Mechanobiology,* vol. 15, no. 4, pp. 915-929, 2015.

[17] K. Reif, S. Gunther, E. Yaz and R. Unbehauen, "Stochastic stability of the discrete-time extended Kalman filter," *IEEE Trans on Automatic Control,* vol. 44, no. 4, pp. 714-728, 1999.

[18] L. Wang, S. Ansari, K. Ward, K. Najarian and K. Oldham, "Identification of compensatory arterial dynamics in swine using a non-invasive sensor for local vascular resistance (under review)," in *Proceedings of the ASME Conference on Dynamic Systems and Control*, Atlanta, GA, 2018.

[19] S. Ansari, M. Tiba, K. Oldham, K. Ward and K. Najarian, "Patterns of oxygen debt repayment during resuscitation of hemorrhage," *Circulation,* vol. 134, no. S1, p. A19409, 2016.